Computers and Electronics in Agriculture 90 (2013) 99–105

Contents lists available at SciVerse ScienceDirect

Computers and Electronics in Agriculture

journal homepage: www.elsevier.com/locate/compag

Automatic classification of non-touching cereal grains in digital images using limited morphological and color features

H.K. Mebatsion, J. Paliwal *, D.S. Jayas

Department of Biosystems Engineering, University of Manitoba, Canada

ARTICLE INFO

Article history:
Received 3 October 2011
Received in revised form 29 August 2012
Accepted 9 September 2012

Keywords:
Machine vision
Cereal grain classification
Automated discrimination

ABSTRACT

Classification of cereal grains, namely; barley, oat, rye and wheat (Canada Western Amber Durum (CWAD) and Canada Western Red Spring (CWRS)) was performed using morphological and color features. Grain image boundary contours were extracted from the digital images of kernels, expressed as chain-coded points and then approximated by 13 elliptic Fourier coefficients. After normalization of the rotation and starting point of the contours, symmetrical standard coefficients were determined. The symmetrical Fourier index (S_{FX}) of individual kernels was calculated from the product of the sum of absolute symmetrical coefficients and the circularity (roundness) index. Three geometric features, namely; aspect ratio (AR), major diameter (M_D) and roundness (C_{eq}) were determined using ellipse fitting and Green's transformation of curve integrals, respectively. The morphological classification model was defined using S_{FX}, AR, M_D, and C_{eq}. The color classification model was defined using color indices of individual kernels, which were calculated from the RGB color values of their images. The classification accuracies of different models were evaluated and compared. The combined model defined by morphological and color features achieved a classification accuracy of 98.5% for barley, 99.97% for CWRS, 99.93% for oat, and 100% for rye and CWAD.

1. Introduction

Grading of cereal grains is important for marketing, efficient handling, transportation, processing, treatment and storage (Hulasare et al., 2003). Grain that are produced and harvested in the field are physically heterogeneous consisting of weeds, inert matter, stones, insects, debris and other grains. The Canadian Grain Council (CGC) defined grading as the segregation of heterogeneous material into a series of grades reflecting different quality characteristics of significance to the users (CGC, 1982). In the Canadian cereal grading system, the main grading factors are: test weight (kg/h L), varietal purity, vitreousness, soundness, and maximum limits of foreign materials (Hulasare et al., 2003). Foreign material is defined as material alien to a particular grain type that is left in a grain lot after cleaning. This could include kernels of other grain types, chaff, stones, broken kernels, etc. (Paliwal et al., 2003). From the grading perspective, it is important to quantify these contaminants in order to assign a fair grade. In this regard, the classification of cereal grains is a crucial component of cereal grading.

With increased research and development and the availability of inexpensive and fast hardware, automatic machine vision systems (MVSs) have become promising technological solutions in the quality evaluation (such as grain purity and absence of broken or damaged kernels) and classification of cereal grains. The MVS for quality control may replace human operators who are subject to external influences such as fatigue, work environment, bias, etc. and make classification and evaluation errors. Other advantages of MVS include results that are objective, repeatable, precise and rapid. Nevertheless, the natural diversity in appearance of various cereal grain varieties makes classification by MVS a complex work to achieve because of the need of a large number of classification features (Douik and Abdellaoui, 2010). Moreover, the anatomical characteristics of cereal grains cannot be defined by unique mathematical functions making the classification process more challenging (Visen et al., 2002).

Available MVS utilize two-dimensional imagery to represent original three-dimensional objects. Such two-dimensional representation poses difficulty in recognizing individual items that touch or overlap with one another in a single image. Touching and overlapping of particles renders the extraction of shape and size parameters very difficult making recognition tasks challenging. Moreover, physical separation of particles using mechanical means prior to imaging is not always practical. These limitations of MVS were the driving forces for the implementation of algorithms that could separate occluding groups of grain kernels in digital images (Mebatsion and Paliwal, 2011; Zhang et al., 2005; Shatadal et al., 1995).

* Corresponding author. Tel.: +1 204 474 8429; fax: +1 204 474 7512.
E-mail address: J_Paliwal@UManitoba.Ca (J. Paliwal).

0168-1699/$ - see front matter © 2012 Elsevier B.V. All rights reserved.
http://dx.doi.org/10.1016/j.compag.2012.09.007

Characterization models based on morphological features (Zapotoczny et al., 2008; Paliwal et al., 2003; Majumdar and Jayas, 2000a), color features (Majumdar and Jayas, 2000b) or textural features (Majumdar and Jayas, 2000c) have been investigated to classify cereal grains. Majumdar and Jayas (2000d) claimed that improved efficiency of classification has been achieved by the combination of these features. Choudhary et al. (2008) integrated wavelet features to further enhance the efficiency of cereal grains classification. Though a high level of classification success was achieved, multiple feature classification models required significantly high number of primary and derived features. Douik and Abdellaoui (2010) and Paliwal et al. (2001) used 152 and 230 morphological, color and textural features, respectively, to attain a near perfect classification of different grain types and dockages. Choudhary et al. (2008) used 335 combined morphological, color, textural and wavelet features to get average classification accuracy of 96%. In this respect, the search for an optimal classification performance with relatively small number of kernel features remains a focus of study because large number of kernel features is a detriment to the classifier's performance (Paliwal et al., 2003). Recent studies by the authors showed that principal component analysis (PCA) of relatively small number of Elliptic Fourier Descriptors (EFDs) could be used to classify cereal grains. Though the segregation of grains based on their shapes was possible, the degree of separation based on EFDs and its potential separation efficiency improvements using some other grain parameters was not investigated. In this regard, the main objectives of this study were: (i) to evaluate the degree of separation of different grains based on indices of elliptic Fourier descriptors (EFDs); and (ii) to develop more robust classification algorithms based on EFDs and additional morphological and color features. In this regard, algorithms based on EFDs and other morphological and color features of barley, oats, rye and wheat (CWAD and CWRS) were developed.

2. Materials and methods

2.1. Grain samples

Five grain types; namely, barley, oats, rye, Canada Western Amber Durum (CWAD) wheat, and Canada Western Red Spring (CWRS) wheat were used in this study. The Industry Services Division of the Canadian Grain Commission (Winnipeg, MB, Canada) provided the grain samples, which were collected at terminal elevators (grain handling facilities). The samples were collected from six locations in Manitoba, 10 locations in Saskatchewan, and six locations in Alberta.

2.2. Imaging and image processing

The images were acquired using a three-chip coupled charge device (CCD) color camera (DXC-3000A, Sony, Japan) with a zoom lens of 10–120 mm focal length (VCL-1012BY), a camera control unit (CCU-M3, Sony, Japan), color frame grabbing and processing boards (DT2871 and DT2858, DATA Translation, Marlboro, MA) and a diffuse illumination chamber. The camera was mounted over the illumination chamber on a stand, which provided easy vertical movement. Illumination was provided by a fluorescent light source of 305 mm diameter, 32-W circular lamp (FC12T9/CW, Philips, Singapore) with a rated voltage of 120 V. The National Television System Committee (NTSC) composite color signal from the camera was converted by the camera control unit at a speed of 30 frames per second into three parallel analogue video signals, namely red (R), green (G) and blue (B), corresponding to the three NTSC color primaries and a synchronous signal. The frame grabber installed in the PC digitized the RGB analogue video signals from the camera control unit into three 8-bit 512 by 480 digital images and stored them in three on-board buffers. The digital images were then sent to the color monitor for on-line display and transferred to a networked storage disk.

Six non-touching grains per grain type were placed on a black board and imaged at a time (Fig. 1). The grain kernels were presorted before the imaging process. The broken, diseased, and discolored kernels were pre-removed and only visually healthy kernels were used. The black board created good contrast between the background and the grain samples and simplified further boundary detection and image processing. The binary images were obtained by thresholding the original digital images. Image processing and boundary detection were carried out in Matlab 7.9 (The Math Works Inc., Natick, MA, USA) using a set of boundary tracing algorithms such as image segmentation, thresholding, edge/boundary detection, and chain coding.

2.3. Data analysis

For cereal grain classification, digital images consisting of 7440, 6918, 7200, 5340, 7200 kernels of barley, CWAD, CWRS, oats, and rye, respectively were used. The testing set consisted of 3716, 3453, 2667, 3599, 3598 kernel images for the respective grains. The rest of the kernel images were used as independent training sets. Image sets of each grain type from a particular geographical location were divided into training and testing sets.

2.4. Morphological features

2.4.1. Geometrical features

The geometric characteristics of individual, non-touching grain kernels were estimated after the transformation of digital images to representative polygons defined by coordinates on the natural boundary of grain kernels. From the resulting coordinates, area (A), perimeter (P), aspect ratio (AR) and major diameter (D_M) were determined using moment calculation and ellipse fitting algorithms. The area and perimeters of approximated polygonal regions were calculated using Green's transformation of curve integrals to line integrals (Mebatsion et al., 2006; Mulchrone and Choudhury, 2004). The aspect ratio of the kernels was estimated using area moments of the best fitting ellipse (Fitzgibbon et al., 1999; Mulchrone and Choudhury, 2004; Mebatsion et al., 2006). The roundness (C_{eq}) of kernels was calculated as $C_{eq} = \frac{4\pi A}{P^2}$.

2.4.2. Fourier coefficient indices

Fourier series approximation of the boundary of kernel shape involves representation of the (x, y) coordinate points into a form of a pair of equations written as a function of a third variable (t). The Fourier coefficients are then calculated based on a discrete Fourier series approximation of chain-coded boundary contours. Individual kernel boundary pixels were used to describe the chain code, starting with a given reference point and tracing the boundary clockwise. Chain-coding was completed when the reference point was reached. The elliptic Fourier series approximation of closed contour projected on the x and y-axes can be defined as follows (Neto et al., 2006; Hiraoka and Kuramoto, 2004; Mebatsion and Paliwal, 2011):

$$x_N(t) = A_0 + \sum_{n=1}^{N} a_n \cos\left(\frac{sn\pi t}{T}\right) + b_n \sin\left(\frac{2n\pi t}{T}\right)$$
$$y_N(t) = C_0 + \sum_{n=1}^{N} c_n \cos\left(\frac{2n\pi t}{T}\right) + d_n \sin\left(\frac{2n\pi t}{T}\right) \quad (1)$$

where t is the step required to move a unit pixel along the closed contour, such that $t_{p-1} < t < t_p$ for $1 \leqslant p \leqslant K$; N is the number of

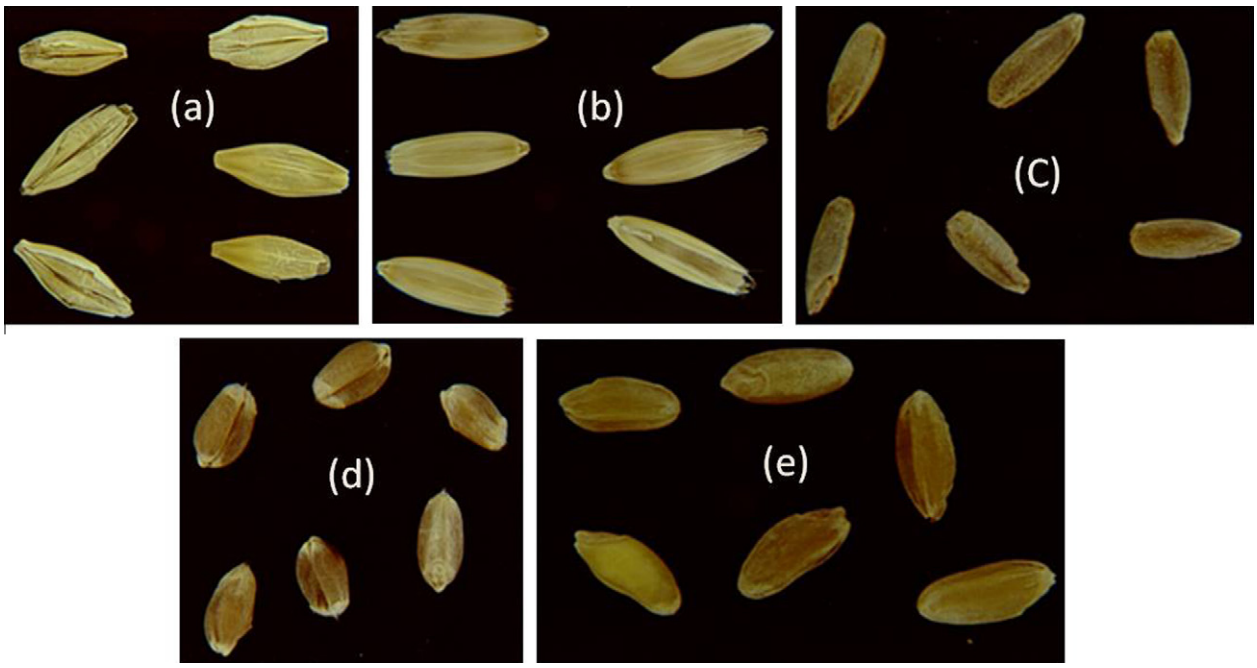

Fig. 1. Non-touching grain imaging. (a) barley; (b) oats; (c) rye; (d) CWRS; and (e) CWAD.

Fourier harmonics; and K is the total number of chain-coded points. A_0 and C_0 are coefficients corresponding to the frequency 0. These coefficients define the mean size of the contour. If the contour between the $(i-1)$-th and the i-th chain-coded points is linearly interpolated and the length of the contour from the starting point to the p-th point and the perimeter of the contour are denoted t_p and T, respectively, then,

$$t_p = \sum_{i=1}^{p} \Delta t_i \tag{1a}$$

T is the basic period of the chain code, which is the overall step to traverse the entire contour, $T = t_k$, where Δt_i is the distance between the $(i-1)$-th and the i-th points. The K-th point is equivalent to the starting point. If the x-coordinate of the p-th point is denoted by x_p, then,

$$X_p = \sum_{i=1}^{p} \Delta x_i, \quad \text{and } y_p = \sum_{i=1}^{p} \Delta y_i \tag{1b}$$

where Δx_i and Δy_i are the distances along the x and y axes between $(i-1)$-th and the i-th point. Assuming linear interpolation between the neighboring points, the elliptic Fourier coefficients in Eq. (1) of the n-th harmonic (a_n, b_n, c_n and d_n) can be calculated using the following equations (Neto et al., 2006; Hiraoka and Kuramoto, 2004; Mebatsion and Paliwal, 2011):

$$\begin{aligned} a_n &= \frac{T}{2n^2\pi^2} \sum_{p=1}^{K} \frac{\Delta x_p}{\Delta t_p} \left(\cos\left(\frac{2n\pi t_p}{T}\right) - \cos\left(\frac{2n\pi t_{p-1}}{T}\right) \right) \\ b_n &= \frac{T}{2n^2\pi^2} \sum_{p=1}^{K} \frac{\Delta x_p}{\Delta t_p} \left(\sin\left(\frac{2n\pi t_p}{T}\right) - \sin\left(\frac{2n\pi t_{p-1}}{T}\right) \right) \end{aligned} \tag{1c}$$

The corresponding coefficients for the y-coordinates, (c_n and d_n) can also be calculated using Eq. (1c) by change of variables. The number of harmonics required to accurately define kernel shape was estimated from average Fourier power spectrum (Costa et al., 2009; Mebatsion and Paliwal, 2011). The Fourier power of a harmonic is proportional to the amplitude and provides a measure of the amount of shape information described by that harmonic. In our study, the Fourier harmonics were truncated at the value $N = 13$, at which the average cumulative power was 99% or more of the total average power (Mebatsion and Paliwal, 2011). The elliptic Fourier coefficients were standardized to make them invariant of the orientation of grains during imaging, and the chain-code starting point on the image contour (Mebatsion and Paliwal, 2011). The Fourier coefficients were normalized based on the ellipse of the first harmonics. The standardized coefficients of the nth harmonic a_{nn}, b_{nn}, c_{nn}, d_{nn}, were calculated as follows:

$$\begin{bmatrix} a_{nn} & b_{nn} \\ c_{nn} & d_{nn} \end{bmatrix} = \begin{bmatrix} \cos\psi & \sin\psi \\ -\sin\psi & \cos\psi \end{bmatrix} \begin{bmatrix} a_n & b_n \\ c_n & d_n \end{bmatrix} \begin{bmatrix} \cos n\theta & -\sin n\theta \\ \sin n\theta & \cos n\theta \end{bmatrix} \tag{2}$$

where

$$\begin{bmatrix} a_{11}^* \\ c_{11}^* \end{bmatrix} = \begin{bmatrix} a_1 & b_1 \\ c_1 & d_1 \end{bmatrix} \begin{bmatrix} \cos\theta \\ \sin\theta \end{bmatrix} \tag{2a}$$

$$\theta = \frac{1}{2} \arctan\left[\frac{2(a_1 b_1 + c_1 d_1)}{(a_1^2 + c_1^2 - b_1^2 - d_1^2)} \right] (0 \leqslant \theta \leqslant \pi) \tag{2b}$$

$$\psi = \arctan\left[\frac{c_{11}^*}{a_{11}^*} \right] (0 \leqslant \psi \leqslant 2\pi) \tag{2c}$$

The elliptic Fourier approximation produces two sets of coefficients that capture the symmetric and asymmetric variations of shapes. The coefficients a_{nn} and d_{nn} represent symmetrical kernel shape variations where as b_{nn} and c_{nn} capture the asymmetrical variations from the central axis of each kernel (Yoshioka et al., 2004). We studied the importance of each group of coefficients in capturing shape variability in grains. The symmetric coefficients captured much of the shape variability in the grains. Hence, the symmetric coefficients and their derivatives were used for classification. From the symmetric elliptic Fourier descriptor, the invariance index (I_{FX}) and the symmetric Fourier index (S_{FX}) were derived as follows:

$$I_{FX} = sqrt(a_{nn}^2 + d_{nn}^2) \tag{3}$$

$$S_{FX} = C_{eq} \times \sum_{nn=1}^{13} abs(a_{nn}) + abs(d_{nn}) \tag{4}$$

The classification potential of EFDs, I_{FX}, and S_{FX} and their combination with AR, C_{eq} and M_D were evaluated.

2.5. Color features

The color features were extracted from the red, green, and blue (RGB) values of the grain images. Then RGB color features were converted into hue, saturation, and value (brightness) (HSV) color system, which is considered closer than the RGB system to the way human eye experiences and interprets color sensation (Gonzalez and Woods, 1992). The conversion from RGB to HSV color system is a matter of developing the equations to map the RGB values (which are Cartesian coordinates) to cylindrical coordinates (Gonzalez and Woods, 1992). Hue describes a pure color (yellow, orange, or red), whereas saturation describes the degree to which a pure color is diluted by white light. Value (brightness) indicates the brightness of the image, and it ranges from black to fully saturated color. The RGB was also converted into Commission internationale de l'éclairage (CIE) L*a*b* system which is a perceptually uniform color space that mimics the logarithmic response of the human eye. The lightness, L*, ranges from 0 (black) to 100 (white), a* ranges from −100 (green) to 100 (red), and b* ranges from −100 (blue) to 100 (yellow). The RGB to CIE L*a*b* color space conversion was carried out according to Connolly and Fleiss (1997).

From the RGB, HSV and CIE L*a*b* color values, the RGBindex (rgb_I), HSVindex (hsv_I), and Labindex (lab_I) were calculated as a square root of the sum of squares of the respective color values. Color values and indices were tested for any significant improvement in performance. If no improvement was observed, they were excluded in the model. In this study, the three-color indices and L and G color values were used as color features for grain classification.

2.6. Least square classifier

The classification of testing sets was achieved by calculating the minimum difference between the morphological or morphological along with color features of the testing sets and that of the training sets. The classification procedure can be summarized as follows. The means and the standard deviations of the morphological and color coefficients of the training sets of barley, oat, rye, and wheat (CWAD and CWRS) kernels were determined. When there was an overlap among the distributions of (morphological, color and morphological along with color) features of the training sets, the classification of a grain kernel was based on the mean feature value. In other words, when the testing set feature values fall within the variation of multiple training sets, the deviation from the mean feature values were used as the main classification factor. Then, for each grain kernel of a specific grain type, the respective parameters were determined. The roots of the square difference of the grain morphological and color coefficients and that of the training sets were calculated. Then, the grain was classified to belong to the training set that gave the least sum of square differences. Fig. 2 shows the graphical representation of the least square classifier. The figure shows alternative classification procedures that we tested. For example, a classification test can be conducted only based on EFD (line 3), or by calculating S_{FX} (line 2) or I_{FX} (line 1). On the other hand, Fourier based morphological parameters can be used along with morphological or color features to perform classification.

The classification accuracy of a classifier (in percentage) was defined as the ratio of the number of grain kernels from the testing set that were correctly classified to the total number of the testing sample of a specific grain type. Classification accuracy, η_c, was given by:

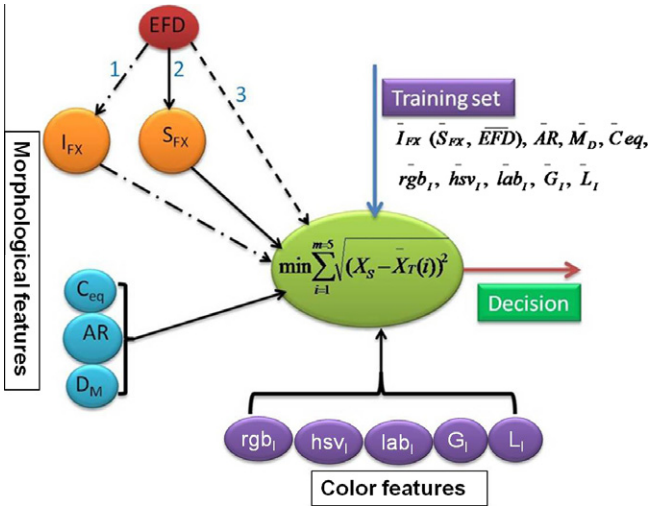

Fig. 2. Least square classification procedure. The variables X_S and X_T represent the testing and training parameters, respectively. The variables with bars on top represent mean values. Broken arrows show alternative combination of shape coefficients used in the classification procedure.

$$\eta_c = \frac{N_{CC}}{N_{TS}} \times 100 \tag{5}$$

where N_{CC} and N_{TS} were defined as the number of grains correctly classified and the total number of testing sets, respectively. η_c Varies between 0 (complete misclassification) and 100% (perfect classification).

3. Results and discussion

The classification results of different models are presented in Tables 1–6. In ideal situation our classifiers classify a specific grain, say barley, with 100% accuracy, which we call perfect classification, based on the characteristics of the training sets. The classifier, however, may classify a certain number of barley kernels from the testing set as barley, CWAD, CWRS, oats or rye. The percentage of barley samples classified as barley, CWAD, CWRS, oats and rye was calculated. The same procedure was repeated for the other grain types and the results were tabulated.

3.1. EFDs based model

Tables 1–3 show the classification accuracies based on S_{FX}, I_{FX}, and EFDs, respectively. The diagonal of the tables shows the percentage of a cereal grain from the testing set classified correctly by a classifier. The S_{FX} model, which is a single coefficient model, achieved the highest classification accuracy for CWRS (100%), followed by oats (99.6%) and CWAD (87.3%) (Table 1). The model had, however, quite limited accuracy for rye kernels (49.3%). It could not differentiate between CWAD and rye and a large

Table 1
Classification of cereal grains based on S_{FX} model. The numbers represent classification accuracies in percentages (%).

	Training set				
Testing set	Barley	CWAD	Oats	CWRS	Rye
Barley	**74.5963**	0.6997	0.0807	0.0269	24.5963
CWAD	11.0918	**87.3154**	0.0000	0.0000	1.5928
Oats	0.1500	0.1500	**99.5876**	0.0750	0.0375
CWRS	0.0000	0.0000	0.0000	**100.0000**	0.0000
Rye	0.7504	49.9166	0.0556	0.0000	**49.2774**

Table 2
Classification of cereal grains based on I_X model. The numbers represent classification accuracies in percentages (%).

	Training set				
Testing set	Barley	CWAD	Oats	CWRS	Rye
Barley	**79.6286**	0.0000	0.0807	0.0000	20.2906
CWAD	0.0000	**67.0432**	12.3661	20.5908	0.0000
Oats	7.3866	0.0000	**77.8778**	0.0000	14.7357
CWRS	0.0000	0.0000	0.0000	**89.4693**	10.5307
Rye	0.1390	0.5837	0.2779	0.0834	**98.9161**

Table 3
Classification of cereal grains based on EFDs model. The numbers represent classification accuracies in percentages (%).

	Training set				
Testing set	Barley	CWAD	Oats	CWRS	Rye
Barley	**79.1981**	0.0269	0.0538	0.0000	20.7212
CWAD	0.0000	**72.8642**	5.9369	21.1990	0.0000
Oats	5.7743	0.0000	**78.1402**	0.0000	16.0855
CWRS	0.0000	0.0000	0.0000	**88.6357**	11.3643
Rye	0.0556	0.6948	0.2501	0.0556	**98.9439**

Table 4
Classification of cereal grains based on color features model. The numbers represent classification accuracies in percentages (%).

	Training set				
Testing set	Barley	CWAD	Oats	CWRS	Rye
Barley	**60.7374**	0.0000	3.8751	35.3875	0.0000
CWAD	0.0290	**99.9710**	0.0000	0.0000	0.0000
Oats	0.0375	0.0000	**99.6250**	0.0375	0.3000
CWRS	51.2365	0.0000	0.0000	**48.7635**	0.0000
Rye	0.0000	0.0000	0.0000	0.0000	**100.0000**

Table 5
Classification of cereal grains based on kernel morphological features model. The numbers represent classification accuracies in percentages (%).

	Training set				
Testing set	Barley	CWAD	Oats	CWRS	Rye
Barley	**91.4155**	0.0000	8.5845	0.0000	0.0000
CWAD	0.0000	**99.971**	0.0000	0.0000	0.0290
Oats	0.0750	0.0000	**99.8875**	0.0000	0.0375
CWRS	0.0000	0.0278	0.0000	**99.9722**	0.0000
Rye	0.0278	0.0000	0.0000	0.0000	**99.9722**

Table 6
Classification of cereal grains based on combined color and morphological model. The numbers represent classification accuracies in percentages (%).

	Training set				
Testing set	Barley	CWAD	Oats	CWRS	Rye
Barley	**98.4661**	0.0000	1.5070	0.0000	0.0269
CWAD	0.0000	**100.0000**	0.0000	0.0000	0.0000
Oats	0.0375	0.0000	**99.9250**	0.0000	0.0375
CWRS	0.0000	0.0278	0.0000	**99.9722**	0.0000
Rye	0.0000	0.0000	0.0000	0.0000	**100.0000**

percentage of rye was misclassified as CWAD (49.9%). However, the classifier precisely differentiated the two wheat types (CWAD and CWRS).

Compared to a one-coefficient S_{FX} model, a 13 coefficients measure, I_X model doubled the separation accuracy of rye kernels to 98.9% (Table 2). On the other hand, the separation accuracies of CWAD, oat and CWRS decreased considerably. With mean separation efficiency of 83.6%, the EFDs model (Table 3) was slightly better than the I_X and S_{FX} models, which had about 82.6% and 82.2% accuracies, respectively. Yet, the separation efficiencies of these approaches are comparatively lower than available models (Majumdar and Jayas, 2000a,b,c,d; Choudhary et al., 2008).

3.2. Color model

Table 4 shows the classification accuracies of the color model defined by five color indices. The model achieved perfect classification accuracy for rye, 99.97% for CWAD and 99.63% for oats. The model, however, gave a very low accuracy for CWRS kernels (48.76%) (Table 4). It could not differentiate between CWRS and barley well. As in the case of S_{FX} model, the classifier precisely differentiated the two wheat types (CWAD and CWRS). The lower classification accuracies of the color model for barley and CWRS indicated the need to have additional parameters included in the model.

3.3. EFDs and geometrical feature model

As we showed in Section 3.1, the separation efficiency of EFD based models did not show any significant difference and hence a one-parameter model based on S_{FX} was used along with other geometrical features. The addition of geometrical features C_{eq}, AR and M_D to the S_{FX} based model improved the classification accuracy for rye, barley and CWAD by 102%, 22.5%, 14.5%, respectively (Tables 1 and 5). The separation accuracy for oats increased by a small percentage, whereas there was no noticeable change in the classification accuracy for CWRS. A comparison of Fourier based and combined classification models are depicted in Fig. 3. The mean separation accuracy of the combined model (equal to 98.2%) is higher than the 97% accuracy obtained by Choudhary et al. (2008). Moreover, our model contained only four morphological features compared to a total of 335 morphological, color, textural and wavelet features used by Choudhary et al. (2008) to achieve comparable accuracies. It is apparent that our EFDs and geometrical feature model with a smaller number of features is more efficient than previously published models. It is a well-documented fact that an unusually large number of classification features increase the complexity of a classifier rendering it computationally expensive and prone to the possibility of over-training (Paliwal et al., 2001)

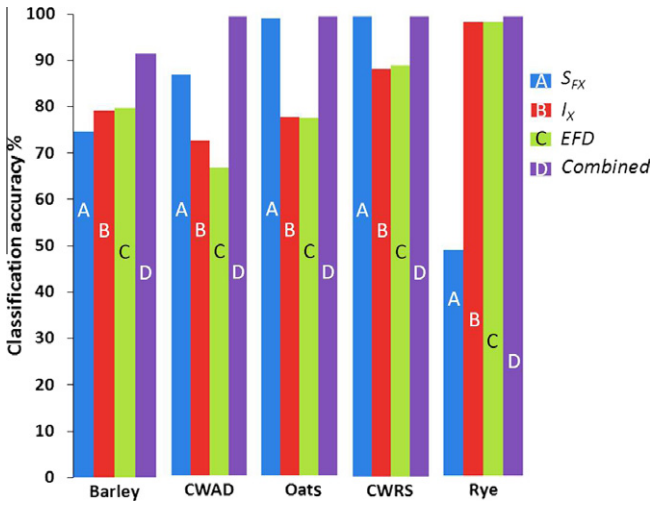

Fig. 3. Comparison of different Fourier based and combined models. S_{FX} represents sum of symmetric Fourier coefficients. I_X is the invariant Fourier coefficient; EFD is the symmetric coefficient model; and morphological model included S_{FX}, AR, D_M and C_{eq}. The combined model contained morphological and color features.

3.4. Combined color and morphological model

Despite a relatively higher classification accuracy of morphological models (containing both EFDs and geometrical features), the results indicated the need to include additional features to get near-perfect classification. In this respect, the morphological and color features combined model achieved perfect classification for CWAD and rye, and near-perfect classification for CWRS and oats (Table 6). The classification accuracy for barley was also very high. With a mean classification accuracy of 99%, our combined model excelled previously published models and our models employed relatively small number of kernel feature inputs (nine inputs). Fig. 3 compares the accuracies of different models. Overall, single-feature classification models show inconsistencies with respect to grain types. The separation accuracy of the grains increased with the addition of geometrical features. The highest consistent accuracy was attained when we used both morphological and color models together.

4. Discussion

As pointed out in the introduction section of this paper, there have been efforts to develop comprehensive machine vision classification algorithms using shape, color, textural features and their combinations with a different degrees of success (Zapotoczny et al., 2008; Paliwal et al., 2003; Majumdar and Jayas, 2000a,b,c,d). However, the number of features involved in the classification and the uniqueness of these features when defined mathematically limited their implementation. This has made researchers invest more time and resources to come up with leaner algorithms consisting of unique features. A good comparison would be the difference observed between this paper and a research paper published by Majumdar and Jayas (2000d). Even though the problem being worked upon is the same, the latter paper is very different in its methodology than what we present in the current paper. Their model employed very large number of color, morphological and textural features, which made the algorithm computationally intensive and hence extremely slow. The aforementioned paper was one of the first attempts to use a comprehensive feature set for cereal grain classification. However, there are several shortcomings that have been identified over the years in their methodology. The morphological features computed by their algorithm were not spatially invariant. The textural features they used viz., gray level co-occurrence matrix (GLCM) and gray level run-length matrix (GLRM) are not very straightforward to calculate. These parameters depend on the choice of 'run-length', which adds another dimension to the complexity of the problem. The RGB color features were weighted and combined in arbitrary proportions to derive secondary statistical features in an almost empirical fashion. All this resulted in a lot of redundancy in the final feature set making it unnecessarily sluggish.

Our approach, in contrast, is a complete departure from their method. We tried to define shape of kernels in terms of IEFDs rather than just length, width, and area type parameters that are dependent on kernel maturity and growing region. While using color, we tried to preserve the fundamental red, green, and blue primaries, as acquired by the camera; rather than creating secondary and tertiary derivative features. This resulted in achieving almost-perfect accuracy with an extremely few features making our algorithm highly computationally efficient for real-time applications.

5. Conclusion

This study established the possibility of classifying cereal grains based on shape defined by Elliptic Fourier Descriptors combined with limited number of geometrical and color features. The results showed that classification based on Fourier descriptors alone was relatively low (83.6%). However, the addition of three geometrical features increased the classification accuracy by about 15% (98.2%). The classification results also showed that our models were more efficient than previously published classification models that involved hundreds of classification features (color, morphological, textural and wavelet features). This was explained by smaller number of classification features for equivalent or even better accuracy. Moreover, the inclusion of color features improved the separation efficiency significantly such that the combined model yielded near-perfect classification for most grain types (>99.9%). Nevertheless, the separation accuracy of the model for barley kernels needs improvement to achieve perfect classification. At this stage, it is reasonable to state that an algorithm now exists that could classify five different cereal grains with near-perfect classification accuracy utilizing only a handful of features. This is in contrast to previously developed algorithms that required hundreds of classification features to attain such high level of accuracies. A separate study is being conducted to develop a learning classifier that will update the training set features from the testing samples during the testing process. We anticipate the learning process will increase the classification accuracy to near perfect level for all of the grain types.

Acknowledgement

We acknowledge the financial support of the Natural Science and Engineering Research Council of Canada (NSERC) and the Canada Research Chairs program.

References

Canada Grains Council (CGC), 1982. Philosophy of grading. In: Grain Grading for Efficiency and Profit. Canada Grain Council, Winnipeg, MB, 6 p.
Choudhary, R., Paliwal, J., Jayas, D.S., 2008. Classification of cereal grains using wavelet, morphological, colour, and textural features of non-touching kernel images. Biosys. Eng. 99, 330–337.
Connolly, C., Fleiss, T., 1997. A study of efficiency and accuracy in the transformation from RGB to CIELAB colour space. IEEE Trans. Image Process. 6 (7), 1046–1048.
Costa, C., Manesatti, P., Pagila, G., Pallottino, F., Aguzzi, J., Rimatori, V., Russo, G., Recupero, S., Recupero, G.R., 2009. Quantitative evaluation of Toroco sweet orange fruit shape using optoelectronic elliptic Fourier based analysis. Postharvest Biol. Tech. 54, 38–45.
Douik, A., Abdellaoui, M., 2010. Cereal grain classification by optimal features and intelligent classifiers. Int. J. Comput. Comm. Contr. 4, 506–516.
Fitzgibbon, A., Pilu, M., Fisher, R.B., 1999. Direct fitting of ellipses. IEEE Trans. Pattern Anal. Machine Intell. 21 (5), 476–480.
Gonzalez, R.C., Woods, R.E., 1992. Digital Image Processing. Addison-Wesley Publishing Co., Reading, MA, USA.
Hiraoka, Y., Kuramoto, N., 2004. Identification of *Rhus succedanea* L. cultivars using elliptic Fourier descriptors based on fruit shape. Silvae Genetica 53 (5–6), 221–226.
Hulasare, R., Jayas, S., Dronzek, B., 2003. Grain grading systems. In: Handbook of Postharvest Technology: Cereals, Fruits, Vegetables, Tea, and Spices, pp. 41–55, doi: 10.1201/9780203911310.ch3.
Majumdar, S., Jayas, D.S., 2000a. Classification of cereal grains using machine vision. I. Morphology models. Trans. ASAE 43 (6), 1669–1675.
Majumdar, S., Jayas, D.S., 2000b. Classification of cereal grains using machine vision. II. Color models. Trans. ASAE 43 (6), 1677–1680.
Majumdar, S., Jayas, D.S., 2000c. Classification of cereal grains using machine vision. III. Texture models. Trans. ASAE 43 (6), 1681–1687.
Majumdar, S., Jayas, D.S., 2000d. Classification of cereal grains using machine vision. IV. Combined morphology, color, and texture models. Trans. ASAE 43 (6), 1689–1694.
Mebatsion, H.K., Paliwal, J., 2011. A Fourier analysis based algorithm to separate touching kernels in digital images. Biosyst. Eng. 108, 66–74.
Mebatsion, H.K., Verboven, P., Verlinden, B., Ho, Q.T., Nguyen, A.T., Nicolaï, B.M., 2006. Microscale modeling of fruit tissue using Voronoi tessellations. Comput. Electron. Agric. 52, 36–48.
Mulchrone, K.F., Choudhury, K.R., 2004. Fitting an ellipse to an arbitrary shape: implications for strain analysis. J. Struct. Geol. 26, 143–153.
Neto, J.C., Meyer, G.E., Jones, D., Samal, A.K., 2006. Plant species identification using elliptic Fourier leaf shape analysis. Comput. Electron. Agr. 50, 121–134.

Paliwal, J., Visen, N.S., Jayas, D.S., 2001. Evaluation of neural network architectures for cereal grain classification using morphological features. J. agric. Engng. Res. 79 (4), 361–370.

Paliwal, J., Visen, N.S., Jayas, D.S., White, N.D.G., 2003. Cereal grain and dockage identification using machine vision. Biosyst. Eng. 85 (1), 51–57.

Shatadal, P., Jayas, D.S., Bulley, N.R., 1995. Digital image analysis for software separation and classification of touching grains. T. ASAE 38 (2), 635–643.

Visen, N.S., Paliwal, J., Jayas, D.S., White, N.D.G., 2002. Specialist neural networks for cereal grain classification. Biosys. Eng. 82 (2), 151–159.

Yoshioka, Y., Iwata, H., Ohsawa, R., Ninomiya, S., 2004. Analysis of petal shape variation of *Primula sieboldii* by elliptic Fourier descriptors and PCA. Annal. Bot. 94, 657–664.

Zapotoczny, P., Zielinska, M., Nita, Z., 2008. Application of image analysis for the varietal classification of barley: Morphological features. J. Cereal Sci. 48, 104–110.

Zhang, G., Jayas, D.S., White, N.D.G., 2005. Separation of touching grain kernels in an image by ellipse fitting algorithm. Biosyst. Eng. 92 (2), 135–142.